NAP-2015

Ethanol Sensing Performances of Zinc-doped Copper Oxide Nano-crystallite Layers

V. Cretu[1], V. Postica[1], N. Ababii[1], F. Schütt[2], M. Hoppe[2], D. Smazna[2], V. Trofim[1],
V. Sontea[1], R. Adelung[2], O. Lupan[1,2]

[1] *Technical University of Moldova, 168 Stefan cel Mare Blvd, MD-2004, Chisinau, Republic of Moldova*
[2] *Functional Nanomaterials, Institute for Materials Science, University of Kiel, D/24143, Germany*

The synthesis via chemical solutions (aqueous) (SCS) wet route is a low-temperature and cost-effective growth technique of high crystalline quality oxide semiconductors films. Here we report on morphology, chemical composition, structure and ethanol sensing performances of a device prototype based on zinc-doped copper oxide nanocrystallite layer. By thermal annealing in electrical furnace for 30 min at temperatures higher than 550 ˚C, as-deposited zinc doped Cu_2O samples are converted to tenorite, $Zn_xCu_{1-x}O_y$, (x=1.3wt%) that demonstrate higher ethanol response than sensor structures based on samples treated at 450 ˚C. In case of the specimens after post-growth treatment at 650 ˚C was found an ethanol gas response of about 79 % and 91 % to concentrations of 100 ppm and 500 ppm, respectively, at operating temperature of 400 ˚C in air.

Keywords: Chemical synthesis, nanocrystalline, ethanol, film, copper oxide, Cu_2O.

PACS numbers: 07.07.Df, 68.47.Gh

1. INTRODUCTION

Ethanol (EtOH), that is also known as ethyl alcohol, is a colorless, flammable, volatile liquid and is extensively utilized in pharmacology, cosmetic production, chemical and food industry, especially in breath analysis and wine-quality monitoring. Ethanol can be used as a fuel for motor vehicles, thus it is an important alternative fuel that produces less greenhouse emission compared to other conventional fuels like methane, propane, etc. Moreover, ethanol consumption is one of the major causes of traffic accidents [1]. In this context appear necessities for monitoring of ethanol vapors to offer safety in homes, vehicles, industry and for detection of the blood alcohol level (BAC) in the body of the drivers [1]. Conventional ethanol sensors are based on oxide semiconductors and are widely used in this domain due to their exceptional properties at nanoscale range, that offer high response, long life cycle, good selectivity, robustness and low cost. Many research activities have been done in the field of ethanol sensors based on oxide semiconductors. One of the most popular among them are *n*-type oxide semiconductors like ZnO [2], SnO_2 [3], WO_3 [4], etc. On the other hand, *p*-type oxide semiconductors like CuO, Cu_2O, NiO, Cr_2O_3, Co_3O_4, etc. have received relatively less attention.

Cuprous oxide (Cu_2O) has been widely studied as a promising material for conversion of the solar energy due to its nontoxicity, low-cost and relatively simple synthesis process [5]. But there are several reports on the ethanol sensing of Cu_2O based sensors with different structures such as combo-like nanorods [6], unifaceted crystals [7], etc. On the other side, cupric oxide (CuO) is known to be an important material in fabrication of high-temperature superconductors [8]. Many researchers have reported that CuO nanostructured films have higher gas response than those of Cu_2O [9]. Thus, it is of practical interest to investigate influence on ethanol gas response of such parameters, like temperature of thermal treatment and operating temperature of device in case of doping of copper oxide films.

Generally, there are only few reports on doped copper oxide based sensors, on Zn-doped CuO in particular are less. A motivation of our research were previous promising results proving that by doping CuO nanorods with Cr it was possible to obtain good selectivity to NO_2 gas [10]. Hübner et. al. has reported that gas response of sensors based on the *p*-type oxide semiconductors is lower than for *n*-type based ones and is equal to the square root of gas response for sensor based on *n*-type oxide semiconductors [11]. Thus, according to previous papers it is more difficult to obtain a *p*-type oxide semiconductor based sensor with a high response.

In current report, we present experimental data on as-grown Zn-doped Cu_2O nanocrystalline films, which were subject of post-growth thermal annealing (TA) in electrical furnace and changed from cuprite phase to cuprite/tenorite phase, then to tenorite crystal phase. Ethanol response of the specimens after different TA treatments and operating temperatures (OPT) was investigated and reported below.

2. EXPERIMENTAL

2.1 Growth of zinc-doped copper oxide nanostructured films

Glass substrates were used for growth of zinc-doped copper oxide nanostructured films by SCS method. The cleaning and synthesis process were reported in our previous work [12]. Thickness of the films is in range of 0.85-0.90 μm as measured in cross-sectional view in scanning electron microscope.

2.2 Characterization

The samples of zinc-doped copper oxide nanostructured films were analyzed using scanning electron microscopy (SEM) instrument Carl Zeiss (7 kV, 10 μA). The compositional analysis of the specimens was carried out by EDX analysis in combination with SEM. Crystallographic information was derived from X-ray powder

diffraction (XRD) data obtained using a Seifert 3000 TT unit operating at 40 kV and 40 mA, with graphite mono-chromatized CuK$_{\alpha1}$ radiation (λ=1.541 Å). Different characterization techniques confirmed that nanostructured films are crystalline. Gas sensing experiments

were performed as reported before [13]. Ethanol gas response was calculated according to relation $S = (\Delta R / R_{air}) \cdot 100$ %, where $\Delta R = R_{EtOH} - R_{air}$, R_{EtOH} is resistance of the sensor under exposure to ethanol vapors and R_{air} is the resistance of sensor in the air.
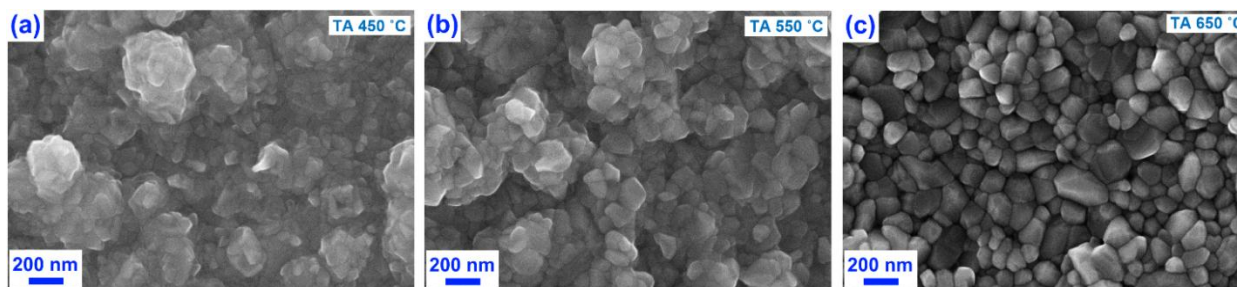

Fig. 1 – SEM images of zinc-doped copper oxide nanostructured films thermally annealed at: (a) 450 ˚C; (b) 550 ˚C; (c) 650 ˚C.
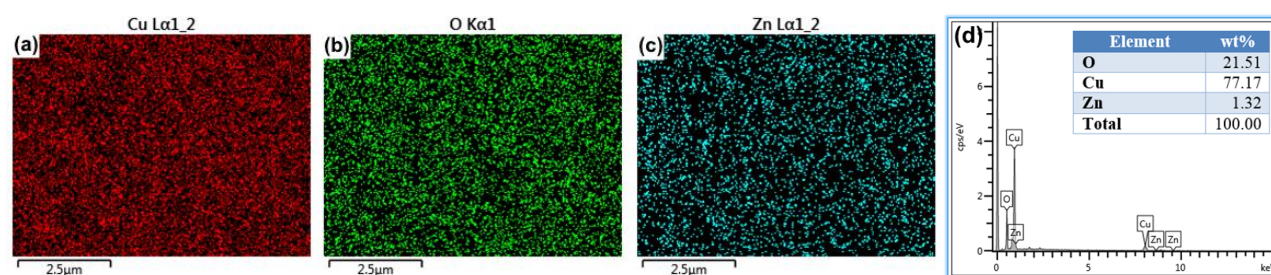

Fig. 2 – Compositional images taken by EDX elemental mapping at the microstructural level of Zn-doped CuO nanostructured films: (a) Cu; (b) O; (c) Zn; and (d) EDX spectrum of Zn-doped copper oxide nanostructured films treated TA at 650 ˚C.

3. RESULTS AND DISCUSSION

In this work we report on morphological, chemical and structural properties of zinc-doped copper oxide nanostructured films TA treated in electrical furnace for 30 min at different temperatures. Also, ethanol vapor response is compared for different values of operating temperatures OPT (300 ˚C, 400 ˚C and 450 ˚C).

3.1 Morphological and Chemical Characterization

In Fig. 1 are presented SEM images of zinc-doped copper oxide nanostructured films grown by SCS and post-growth treated TA at (a) 450 ˚C, (b) 550 ˚C and (c) 650 ˚C. Films are relatively uniform on substrate and are composed of interconnected nanocrystallites with diameter in range of 50 – 200 nm, depending on regime. It can be observed that crystallinity and diameter of nanocrystallites increased with the temperature of TA. Thus, samples treated at 650 ˚C (see Fig. 1c) have larger nanocrystallites than specimens annealed at 450 ˚C or 550 ˚C (see Fig. 1a-b). In result, surface-to-volume ratio was increased and it affects sensing properties.

Fig. 2a-c presents compositional images taken by EDX elemental mapping at the microstructural level of Zn-doped CuO. The uniform distribution of elements Cu, O and Zn-dopant is clearly seen in the film of the nanostructures used in our sensor studies. Fig. 2d reveals an EDX spectrum of Zn-doped copper oxide nanostructured films treated TA at 650 ˚C for 30 min. Cu and O can be distinguished from copper oxide film. Incorporation of zinc dopant is confirmed by Zn peaks in EDX spectrum. Zinc content in copper oxide

nanostructured films treated TA at 650 ˚C was found to be as low as 1.32 wt% in different regions.

3.2 Structural Characterization

Structural properties of the thermal annealed TA samples were investigated by X-ray diffraction technique (XRD). In previous work [14] is demonstrated that as deposited Zn-doped CuO nanostructured films possess the cuprite phase. Fig. 3 shows the XRD patterns of the zinc-doped copper oxide nanostructured films treated TA at 450 ˚C, 550 ˚C and 650 ˚C for 30 min, recorded in the two theta range of 20-100˚. The peaks were observed that correspond to simple cubic Cu$_2$O (cuprite JCPDS # 00-050-0667, see curve 1) and monoclinic CuO (tenorite JCPDS # 00-045-0937, see curves 1-2-3).
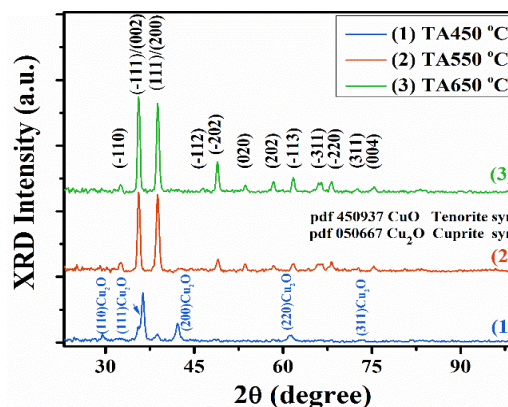

Fig. 3 – XRD patterns of the Zn-doped copper oxide nanostructured films treated TA at 450 ˚C, 550 ˚C and 650 ˚C for 30 min.
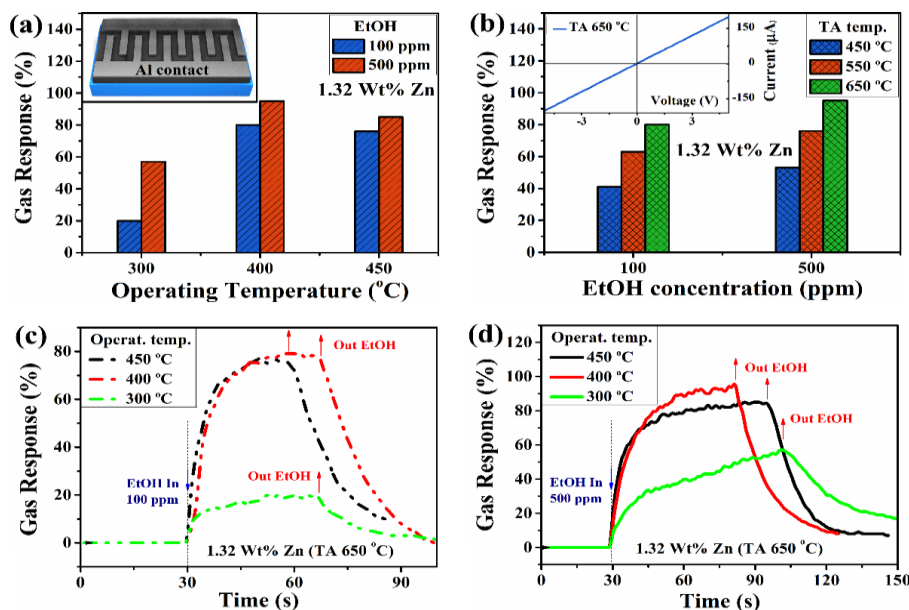
Fig. 4 – Gas response to ethanol vapors of zinc-doped copper oxide nanostructured films based sensor versus: (a) Operating temperature for 100 ppm and 500 ppm EtOH, treatment regime TA was at 650 ˚C for 30 min; (b) concentration of EtOH for different temperature of treatment TA in electrical furnace. Dynamic response to ethanol of zinc-doped copper oxide nanostructured films based sensor versus operating temperature and concentration of EtOH: (c) 100 ppm; and (d) 500 ppm.

Peaks that correspond to the Zn impurities are not observed in XRD patterns, that indicate incorporation of Zn ions into the lattice of copper oxide without changes in structural properties [15], see Fig. 3. Also peaks that correspond to $Cu(OH)_2$ or Cu were not observed in diffractograms. In the case of sample treated TA at 450 ˚C (Fig. 3, curve 1) mixed phase is observed and the dominant phase is cuprite. The characteristic peaks at 36.3˚, 42.4˚ and 61.6˚ correspond to reflections from (111), (200) and (220) planes, respectively. In the case of samples treated in air at 550 ˚C and 650 ˚C the peaks have been observed that corresponds only to tenorite phase. Nair et al. [16] demonstrate that as-deposited Cu_2O films by chemical method converts to CuO phase at temperatures higher than 350 ˚C. Improved crystallinity of the Zn-doped copper oxide films with increasing TA temperature, observed in the SEM images (see Fig. 1) has been confirmed by XRD measurements by appearance of stronger peaks for samples treated at 650 ˚C.

3.3 Ethanol Vapor Response

Fig. 4a unveils gas response of sensors based on 1.3 wt% zinc-doped copper oxide nanostructured films to ethanol versus OPT and concentration of ethanol vapors. The inset schematically represents the structure of sensor investigated in this research. Aluminum (Al) contacts are deposited by evaporation in vacuum using an Al mask with meander configuration. Width of meander was 1 mm. Type of formed contacts are one of the most important factors that control the sensing properties of oxide semiconductor sensors. The current-voltage characteristics of sensor structures based on zinc-doped copper oxide nanocrystalline films treated TA at 650 ˚C is presented in inset of Fig. 4b, and it demonstrates the linear behavior indicating Ohmic contacts. Theoretically Al contacts form a Schottky barrier with *p*-type copper oxide, due to lower work function of Al, which was experi-

mentally demonstrated by Ushio et al. [17]. In our case, formation of Ohmic contacts is probably due to defects at the Al/CuO:Zn interface or due to the doping effect. The Ohmic behavior ensures that sensors signal is not influenced by the contacts between Al layer and zinc–doped CuO nanostructured film, but is originating only from sensing layer [18]. Optimal operating temperature OPT was found to be at about 400 ˚C for both concentration of ethanol vapors (see Fig. 4a). Also was investigated dependence of ethanol gas response on temperature of postgrowth treatment TA (see Fig. 4b). In the presence of mixed phase of cuprite/tenorite gas response was lower ~ 40 % for 100 ppm and ~ 52 % for 500 ppm (sample set TA 450 ˚C). For sensors based only on the tenorite phase gas response was found to be higher ~ 79 % for 100 ppm and about 91 % for 500 ppm (sample set TA 650 ˚C), that is higher than for the sample treated at 550 ˚C, probably due to lower crystallinity of Zn-doped CuO films treated at 550 °C and a higher surface-to-volume ratio for sample Zn-doped CuO films treated at 650 ˚C. Barreca et al. [19] and Zoolfakar et al. [9] demonstrate that ethanol response of sensors based on CuO film is higher than for sensors based on Cu_2O. One of the reasons can be different type of reaction at the surface of nanocrystallites that include a different type of sensing mechanism. Further possible sensing mechanisms of ethanol sensors based on copper oxide nanostructured films will be discussed.

In Fig. 4c and 4d are presented dynamic responses to ethanol 100 ppm and 500 ppm, respectively, of sensor structures based on zinc-doped copper oxide nanostructured films. The response time of sensors at OPT 400 ˚C and 450 ˚C was ~ 15 s, and at 300 ˚C of 30 − 40 s. The recovery time was much higher, in range of 35 − 50 s for OPT 400 ˚C and 450 ˚C, while for OPT 300 ˚C it was higher than 60 s.

It is well known, that at high temperatures oxygen interacting with surface of oxide semiconductors by the following equations [20]:

$$\frac{1}{2}O_{2(g)} \leftrightarrow O_{(ad)} \qquad (3.1)$$

$$O_{(ad)} \leftrightarrow O'_{(ad)} + h^+ \qquad (3.2)$$
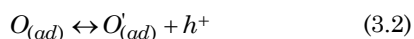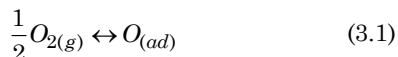
Thus, oxygen atom, after adsorption on copper oxide surface, has left a hole (h^+) in the lattice, forming the hole accumulation layer (HAL) on a surface of nano-crystalline film. Resistance of this layer is much lower than the one of the insulating core. After exposure to reducing gas, in our case to ethanol vapors, the concentration of electrons in HAL will increase, that result in recombination of electron-holes and in a narrowing of HAL [21]. Thus, the resistance of sensor structure will increase after exposure to ethanol vapors due to reduction of charge carriers' concentration. Interaction of adsorbed oxygen species on surface of copper oxide semiconductor with ethanol molecules can be described by the following equation [22]:

$$C_2H_5OH_{(g)} + 6O^-_{(ad)} + 6h^+ \rightarrow 2CO_{2(g)} + 3H_2O_{(g)} \quad (3.3)$$
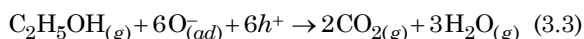
In results of equation (3.3), via interaction of one molecule of ethanol with six ions of oxygen on the surface, recombination of six holes from HAL with six electrons released by desorbed species on surface occurs. Another important factor that need to be taken into account is surface band bending V_S between nanocrystallites. The conductance of ethanol gas sensor structure based on zinc-doped copper oxide nanocrystallite films is dependent of V_S value by the following equation [11]:

$$G_p \approx \exp(qV_S/2kT) \qquad (3.4)$$

In results of equation 3.3, value of V_S will be modified and gas response will be determined by ΔV_S [11], where $\Delta V_S = V_{S\ air} - V_{S\ EtOH}$, $V_{S\ air}$ − is value of band bending in air and $V_{S\ EtOH}$ − is value of band bending under exposure to ethanol vapors in air. General de-pendence of the response is represented by [11]:

$$S = \exp(-q\Delta V_S/2kT) \qquad (3.5)$$

In our case, a higher ethanol response of sensors based on the zinc-doped copper oxide nanostructured films could be due to nanocrystallites shapes that result in higher volume-to-surface ratio, and in more barriers which are formed between them. In such a case, larger amount of gas molecules is adsorbed on surface of nanostructured zinc doped copper oxide, which produces a higher gas response.

4. CONCLUSIONS

We have demonstrated doping of copper oxide nano-crystalline films with zinc by SCS method at a relatively low temperature. High crystallinity of samples was detected by the XRD studies. Sensors based on these films shows good response to ethanol vapor in concentrations of 100 ppm and 500 ppm at $300-450$ ˚C operating temperatures. The highest gas response of around 80 % to 100 ppm ethanol and of approximately 95 % to 500 ppm ethanol was obtained for films treated TA at 650 ˚C for 30 min, which demonstrates presence of only tenorite phase. Values of response time and recovery time were found to be dependent on operating OPT value due to temperature dependency of adsorption/desorption coefficient. Also, the value of ethanol response was decreased with lowering temperature of annealing TA down to 450 ˚C. In results, according to these experimental data, the tenorite phase of copper oxides is more sensitive to ethanol vapors than cuprite or cuprite/tenorite mixed phases.

REFERENCES

1. *Sensors for Chemical and Biological Applications* (Ed. M. K. Ram, V. R. Bhethanabotla) (Taylor & Francis Group, LLC: 2010).
2. Q. Wan, Q.H. Li, Y.J. Chen and T.H. Wang, *Appl. Phys. Lett.* **84**, 3654 (2004).
3. Y.J. Chen, X.Y. Xue, Y.G. Wang, T.H. Wang, *Appl. Phys. Lett.* **87**, 233503 (2005).
4. D. Chen, X. Hou, H. Wen, Y. Wang, H. Wang, X. Li, R. Zhang, H. Lu, H. Xu, S. Guan, J. Sun, L. Gao, *Nanotechnology* **21** 035501 (2010).
5. A.O. Musa, T. Akomolafe, M. J. Carter, *Solar Energ. Mater. Sol. Cells* **51** 305 (1998).
6. L. Guan, H. Pang, J. Wang, Q. Lu, J. Yin, F. Gao, *Chem. Commun.* **46**, 7022 (2010).
7. K.X. Yao, X.M. Yin, T. H. Wang, H. C. Zeng, *J. Am. Chem. Soc.* **132**, 6131 (2010).
8. P. Raksa, A. Gardchareon, T. Chairuangsri, P. Mangkorntong, N. Mangkorntong, S. Choopun, *Ceram. Inter.* **35**, 649 (2009).
9. A.S. Zoolfakar, M.Z. Ahmad, R.A. Rani, J.Z. Ou, S. Balendhran, S. Zhuiykov, K. Latham, W. Wlodarski, K. Kalantar-zadeh, *Sensor. Actuat. B-Chem.* **185**, 620 (2013).
10. K.-M. Kim, H.-M. Jeong, H.-R. Kim, K.-I. Choi, H.-J. Kim, J.-H. Lee, *Sensors* **12**, 8013 (2012).
11. M. Hübner, C. E. Simion, A. Tomescu-Stănoiu, S. Pokhrel, N. Barsan, *Sensor. Actuat. B-Chem* **153**, 347 (2011).
12. V. Creţu, V. Postica, N. Ababii, V. Şontea, O. Lupan, *8th International Conference on Microelectronics and Computer Science*, 106 (2014).
13. O. Lupan, G. Chai, L. Chow, *Micro.. Eng.* **85**, 2220 (2008).
14. V. Creţu, N. Ababii, V. Postica, V. Sontea, V. Trofim, S. Railean, I. Pocaznoi, O. Lupan, *II-Th Regional Workshop Health Technology Management*, 72 (2014).
15. T.V. Thi, A.K. Rai, J. Gim, J. Kim, *Appl. Surf. Sci.* **305**, 617 (2014).
16. M.T.S. Nair, L. Guerrero, O.L. Arenas, P.K. Nair, *Appl. Surf. Sci.* **150**, 143 (1999).
17. Y. Ushio, M. Miyayama, H. Yanagida, *Sensor. Actuat. B-Chem.* **12**, 135 (1993).
18. G. Zhu, H. Xu, Y. Xiao, Y. Liu, A. Yuan, X. Shen, *ACS Appl. Mater. Interfaces* **4**, 744 (2012).
19. D. Barreca, E. Comini, A. Gasparotto, C. Maccato, C. Sada, G. Sberveglieri, E. Tondello, *Sensor. Actuat. B-Chem.* **141**, 270 (2009).
20. A. Cruccolini, R. Narducci, R. Palombari, *Sensor. Actuat. B-Chem.* **98**, 227 (2004).
21. V.B. Kamble, A. M. Umarji, *J. Mater. Chem. C.* **1**, 8167 (2013).
22. Y.-H. Choi, D.-H. Kim, S.-H. Hong, K.S. Hong, *Sensor. Actuat. B-Chem.* **178**, 395 (2013).